Ionics (2023) 29:625–638
https://doi.org/10.1007/s11581-022-04857-0

ORIGINAL PAPER

Ionic transport study of hybrid gel polymer electrolyte based on PMMA-PLA incorporated with ionic liquid

N. F. Mazuki[1] · K. Khairunnisa[1] · M. A. Saadiah[2] · M. Z. Kufian[3] · A. S. Samsudin[1]

Received: 13 October 2022 / Revised: 22 November 2022 / Accepted: 5 December 2022 / Published online: 15 December 2022
© The Author(s), under exclusive licence to Springer-Verlag GmbH Germany, part of Springer Nature 2022

Abstract

Hybrid gel polymer electrolytes (HGPEs) based on polymethyl methacrylate (PMMA)-polylactic acid (PLA) doped with LiTFSI and incorporated with 1-butyl-3-methylimidozalium chloride (BmimCl) were successfully prepared. The complexes of the HGPEs with different BmimCl contents were characterized via Fourier transform infrared (FTIR) and X-ray diffraction (XRD) analysis. Based on the impedance spectroscopy analysis, the HGPEs with the composition of 80% PMMA:20% PLA:20 wt.% LiTFSI:15 wt.% BmimCl possessed the highest room-temperature ionic conductivity of 1.63×10^{-3} S cm^{-1}. The Arof-Noor (A-N) method was applied to investigate its transport properties, and it was found that the diffusion coefficient, D, ionic mobility, μ, and number density of ions, η, were the main contributors of ionic conductivity improvement. Meanwhile, the highest conducting electrolyte lithium ion transference number was 0.67. Linear sweep voltammetry (LSV) analysis showed that the electrochemical stability window of the HGPE was 3.4 V vs Li/Li$^+$. The findings suggest that the HGPE system incorporated with this ionic liquid could be a promising candidate for use as an electrolyte in flexible lithium-ion batteries.

Keywords Ionic liquid · Lithium transference number · Potential stability · Hybrid polymer

Introduction

With the development of advanced technologies, lithium-ion batteries are identified as the most promising and suitable candidate for developing new-generation energy vehicles. Lithium-ion batteries offer attractive performance characteristics, including a high-temperature range of operation, large capacity, high power and energy density, low rate of self-discharge, rapid charge capability, and relatively longer charge–discharge life [1–5]. Moreover, lithium-ion batteries can also be designed to be lighter and smaller in weight and size, which meets the commercial demand [6]. However, safety issues have arisen, as most lithium-ion batteries use liquid organic solvents in their electrolytes that can cause leakages, thus could lead to an explosion [7]. To address these issues, polymer electrolytes (PE) are being proposed to replace liquid electrolytes. Fenton et al. were the first to fabricate a PE in 1973, which composed of salts dissolved in a polymer [8]. Since then, PE have drawn much attention among researchers due to its potential applications in lithium-ion batteries and other electrochemical devices such as supercapacitors, solar cells, and fuel cells.

In general, PE can be divided into three types based on their physical appearance and composition: (a) solid polymer electrolytes (SPE) [9]; (b) gel polymer electrolytes (GPE) [10]; and (c) composite polymer electrolytes (CPE) [11]. Several criteria of polymer electrolytes must be considered for energy storage applications. They include high ionic conductivity over a wide range of temperatures (10^{-3} to 10^{-2} S cm^{-1}), good mechanical strength, wide potential stability window, good contact with the electrode, and low cost [12–15]. Among the three PE types, gel polymer electrolytes (GPEs) are suggested as the most promising candidate for application in lithium-ion batteries. GPEs possess both the

✉ A. S. Samsudin
ahmadsalihin@ump.edu.my

[1] Ionic Materials Team, Faculty of Industrial Sciences and Technology, Universiti Malaysia Pahang, 26300 Gambang, Pahang, Malaysia

[2] Department of Chemistry, Centre for Foundation Studies, International Islamic University Malaysia, 26300 Gambang, Pahang, Malaysia

[3] Centre for Ionics University of Malaya, Department of Physics, Faculty of Science, Universiti Malaya, 50603 Kuala Lumpur, Malaysia

cohesive properties of a solid and the diffusive properties of a liquid, allowing them to achieve high room temperature ionic conductivity compared to SPEs and CPEs. Yet, GPEs suffer from poor mechanical strength and thermal stability that may lead to internal short-circuiting due to bad electrode/electrolyte contact [16].

Consequently, several approaches have been developed in the preparation of GPEs to improve the electrolyte's performance, such as blending polymers [17], doping with inorganic fillers [18], addition of ionic liquids (IL) [19], and physical/chemical cross-linking [20]. According to Pan et al. [21], the ionic conductivity and mechanical properties of GPEs can be improved by blending a single host polymer with another polymer. Polymethyl methacrylate (PMMA), polyethylene oxide (PEO), polyvinylidene fluoride (PVDF), and polyvinylidene fluoride-hexafluoro propylene are the most common host polymers used in GPEs application. PMMA is a vinyl polymer known as an ester of methacrylic acid ($CH_2=C[CH_3]CO_2H$) groups. The pendant CH_3 group in the PMMA structure hinder the crystalline packing and allow ions to move freely around the C–C bonds [22]. Kuppu et al. [23] reported the highest room temperature ionic conductivity of 4.62×10^{-3} S cm^{-1} for their polymer blend-based PMMA-PVDF-Al_2O_3-KI GPEs. Ramesh et al. [24] also reported that their polymer blend-based PMMA-PVC GPEs had a maximum ionic conductivity at 8.08×10^{-4} S cm^{-1} with 60 wt.% BmImTFSI. Based on these previous findings, it was noted that the ionic conductivity values increased gradually when PMMA was blended with another polymer compared to pure PMMA which has ionic conductivity values of $\leq10^{-12}$ S cm^{-1} [25]. Moreover, the introduction of polylactic acid (PLA) into PMMA allowed the manipulation of the polymer structure via dipole–dipole interaction. It enhanced the conduction mechanism by providing more vacancies for ions to migrate in the polymer backbone [26].

Many studies reported that GPEs containing different ILs offer outstanding physical and electrochemical properties for applications in lithium-ion batteries [27–29]. ILs possess many unique properties, such as expansive electrochemical windows, high thermal stability, low vapor pressure, high viscosity, being non-flammable, and non-volatile [30, 31]. Balducci et al. found that ILs may also enhance the ionic conductivity by increasing the number of charge carriers without negatively affecting the mechanical stabilities of the electrolytes [32]. Among promising ILs, BmimCl has been widely investigated as a precursor in polymer electrolytes [33–36].

Therefore, the present work investigated the enhancement of hybrid gel polymer electrolyte-based PMMA-PLA by incorporating different amounts of BmimCl as the ionic liquid. This work aims to study the effects of BmimCl on the electrical and physiochemical properties of HGPE systems using impedance spectroscopy, FTIR, and XRD analysis. These IL-based HGPEs demonstrated significantly enhanced ionic conductivity due to the rise in mobile ions which then interacted with the oxygen group from the host polymer backbone via dipole–dipole interaction, hence facilitating ion transport. The ionic transport properties were thus studied to understand the principles of the HGPE system. Furthermore, the highest conducting electrolyte was then chosen to measure the lithium transference number and potential window stability.

Experimental

Materials

PMMA with a molecular weight of 996,000 and PLA with a molecular weight of 120,000 were purchased from Aldrich Co. and Shandong Zhi Shang Chemical Co. LTD, respectively. Lithium bis(trifluoromethanesulfony)imide (LiTFSI) was obtained from Aldrich Co. The solvent tetraethylene glycol dimethyl ether (TEGDME) was bought from Acros Organic, while molecular sieve (4 Å) and BmimCl were both sourced from Sigma Aldrich and Aldrich, respectively.

Preparation of IL-based hybrid gel polymer electrolytes

Our previous work [25] showed that the 80:20 ratio of PMMA:PLA incorporated with 20 wt.% LiTFSI-based HGPE exhibited the highest ionic conductivity at room temperature and this composition was chosen in the present study for further enhancement by adding an IL into the solution. IL-based HGPEs were prepared by dissolving PMMA, PLA, LiTFSI, and BmimCl in TEGDME. Firstly, PLA was added to TEGDME and vigorously stirred at 120 ℃ until it completely dissolved. Then, 20 wt.% of LiTFSI was introduced into the PLA solution and mixed at room temperature. After the solution was completely homogenous, different ratios in weight percentage of BmimCl, from 5 to 30 wt.%, were incorporated into the PLA-LiTFSI solution with continuously stirring at room temperature. PMMA was the last compound added into the mixed solution which was constantly stirred with open heat at 70 ℃ until a gel was formed. The prepared PMMA-PLA-LiTFSI-BmimCl HGPEs was suctioned with a vacuum pump and stored in an argon atmosphere before further testing.

Characterization

FTIR spectroscopy measurements

Fourier transform infrared spectroscopy (FTIR) was used in the present study to investigate the possible interaction of PMMA-PLA-LiTFSI polymer electrolyte with BmimCl. The

analysis was performed using a Nicolet 6700 Thermo-Fisher Scientific FT-IR, fitted with an Attenuated Total Reflection (ATR) accessory with a zinc selenide (ZnSe) crystal. The electrolytes were measured at a wavenumber range of 4000 to 700 cm^{-1} with a scanning resolution of 2 cm^{-1}.

XRD measurements

The X-ray diffraction (XRD) analysis was carried out using a Rigaku MiniFlex II Diffractometer equipped with a nickel filtered C_uK_α ($\lambda = 0.154$ nm) uplifted at 30 kV, and 15 mA. The data were collected from a diffraction angle of 2θ in the range of 5° to 80° to investigate the crystallinity and amorphousness of the sample.

Electrical impedance spectroscopy studies

The complex impedance measurement was evaluated by using alternating current (ac) impedance spectroscopy on a HIOKI 3532–50 LCR Hi-TESTER with an ac amplitude of 10 mV from 1 MHz to 50 Hz. In determining the impedance measurement, the IL-based HGPE was positioned into the stainless-steel (SS) coin cell to control the diameter of the sample. The setup can be referred to from our previous work [26]. The ionic conductivity at room temperature was determined using bulk electrolyte resistance (R_b) gained from the Cole–Cole plot as presented in the following relation:

$$\sigma = \frac{T}{R_b A} \tag{1}$$

where T is thickness of the electrolyte, while A is the contact area between the electrolyte and the SS disc.

Lithium-ion transference measurement number studies

The lithium-ion transference number (t_{Li}^+) for the current system was examined according to the Bruce and Vincent method [37–39], which uses a combination of ac impedance spectroscopy and direct current (dc) polarization technique. The IL-based HGPE was sandwiched between two lithium metal electrodes in the Li|IL-based HGPE|Li cell configuration. When a constant polarization current (100 mV) was applied to the electrodes of the cell, a current was measured that fell from an initial (I_o) value to a steady-state (I_{ss}) value. The t_{Li}^+ was calculated with the following formula:

$$t_{Li}^+ = \frac{I_{ss}(\Delta V - I_o R_o)}{I_o(\Delta V - I_o R_o)} \tag{2}$$

where ΔV is the potential applied across the cell. R_o and R_{ss} are, respectively, the interfacial resistance at the initial and steady states. The interfacial stability of the IL-based HGPE was investigated using ac on a Gamry Instrument EIS with an ac amplitude of 100 mV from 100 kHz to 1 Hz at room temperature.

Linear sweep voltammetry

The electrochemical stability of IL-based HGPE was investigated in a cell arrangement of Li|IL-based HGPE|SS via linear sweep voltammetry LSV at 10 mV s^{-1}.

Results and discussion

FTIR analysis

Figure 1 presents the FTIR spectra of PMMA-PLA-LiTFSI and various contents of BmimCl-based HGPEs at the selected region of 3200–2700 cm^{-1} and 1900–1500 cm^{-1}. It can be seen from Fig. 1(i) that the stretching frequency at 2877 cm^{-1} corresponding to the C-H of the host hybrid polymer PMMA-PLA were broadened when the IL was introduced into the system, up to 10 wt.% BmimCl. The C-H bond, known as the tertiary C-H group, can explain the reduction of peak intensity at this region, where they easily break and are lost to other aliphatic C-H absorptions in the polymer complex [40]. It was also noticed that a new peak was observed at 2950 cm^{-1} at high contents of BmimCl, which might be due to the overlapping of the C-H vibration mode for cyclic $Bmim^+$ [33]. A similar observation was found in a previous work by Latifi et al. [35], where they claimed the presence of a new peak indicates increased IL content because of the C-H symmetric stretching mode in the methyl group of the alkyl chain and imidazolium rings of BmimCl.

The C=O stretching bands of HGPE without IL (0 wt.% BmimCl) were found at 1729 cm^{-1}, as shown in Fig. 1(ii). It can be observed that the bands broadened with the incorporation of BmimCl. This indicates that a complexation has occurred due to the C=C stretching of the imidazolium ring [35]. Ghani et al. [41] reported that all the hydrogen atoms in the imidazolium ring have the potential to interact with the polymer host via hydrogen bonding. Therefore, the change in peak intensity of the ester group (C=O) stretching might be due to the oxygen molecule from the host hybrid polymer interacting with the imidazolium ring's hydrogen group. In addition, the addition of IL beyond 5 wt.% to the PMMA-PLA-LiTFSI system led to the appearance of new peaks at 1570 cm^{-1}, which are assigned to the C=N stretching mode of BmimCl. The transmittance of the C=N peak intensity also increased as more BmimCl was added, and this might be due to the presence of the imidazole cation in the IL-based HGPE systems [34].

The band at 1454 cm^{-1} was assigned to the CH_3 bending mode of PMMA-PLA hybrid polymer as shown in Fig. 2(i).

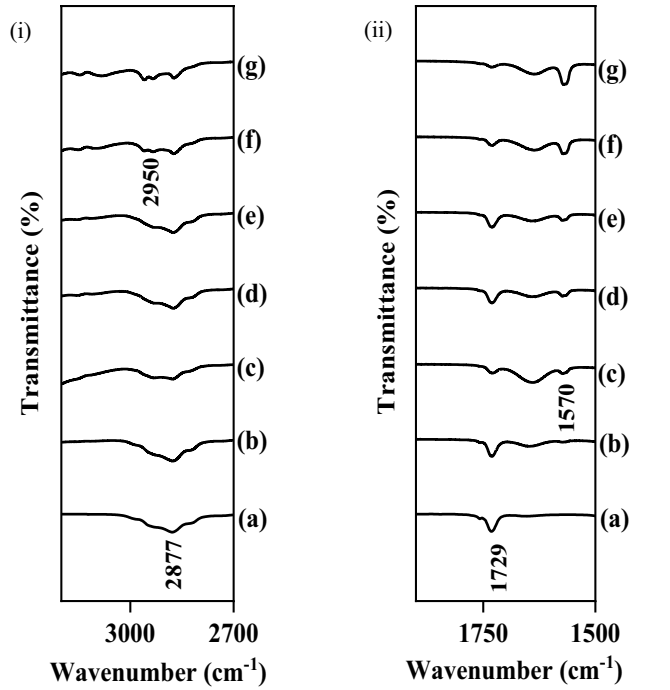

Fig. 1 IR spectra of (a) PMMA-PLA-LiTFSI (0 wt.% BmimCl), (b) 5 wt.% BmimCl, (c) 10 wt.% BmimCl, (d) 15 wt.% BmimCl, (e) 20 wt.% BmimCl, (f) 25 wt.% BmimCl, and (g) 30 wt.% BmimCl at highlighted region covering wavenumber of (i) 3200–2700 cm^{-1} and (ii) 1900–1500 $cm.^{-1}$

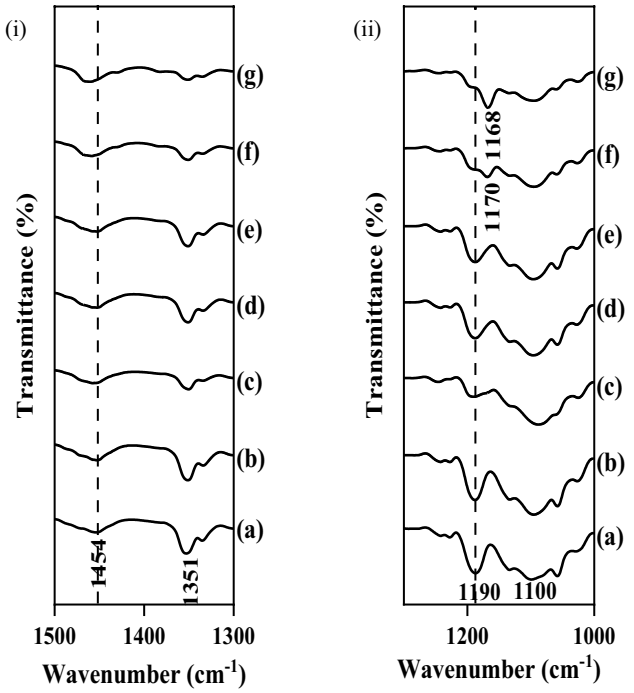

Fig. 2 IR spectra of (a) PMMA-PLA-LiTFSI (0 wt.% BmimCl), (b) 5 wt.% BmimCl, (c) 10 wt.% BmimCl, (d) 15 wt.% BmimCl, (e) 20 wt.% BmimCl, (f) 25 wt.% BmimCl, and (g) 30 wt.% BmimCl at highlighted region covering wavenumber of (i) 1500–1300 cm^{-1} and (ii) 1300–1000 $cm.^{-1}$

However, the presence of 25 wt.% and 30 wt.% of BmimCl have shifted the characteristic band to higher wavenumbers. It was also observed that the peak intensity was increased at high ionic liquid contents. The shift in wavenumbers and peak intensity are probably attributed to the overlapping of the CH_2 symmetric bending mode from the IL. Another obvious change of peak intensity was observed at 1351 cm^{-1} which proved the occurrence of complexation when BmimCl was introduced into HGPE system. The peak for the CH_2 symmetric bending mode slowly became wider, while the transmittance intensity was reduced as more IL was incorporated into the system.

From our previous work [26], a sharp peak at 1190 cm^{-1} was assigned to the CF_3 symmetric stretching mode of LiTFSI as shown in Fig. 2(ii). On the addition of 25 wt.% BmimCl, the band shifted to lower wavenumbers, from 1190 to 1170 cm^{-1}. The peak shifted to 1168 cm^{-1} with the incorporation of 30 wt.% BmimCl. It is suggested that this phenomenon was due to the increasing IL content, and the CH_3-N stretching mode of BmimCl slowly taking place at that region [33]. Furthermore, the CH_3-N group from BmimCl dominated in the HGPE system and removed the CF_3 band of LiTFSI when the amount of BmimCl was more than LiTFSI. The FTIR spectra of the IL-based HGPE systems in the C–O–C stretching vibration region are shown in Fig. 2(ii). A wide band was detected at 1100 cm^{-1} in the wavenumber range of 1300 to 1000 cm^{-1}, which was assigned as the C-O stretching of HGPEs. The transmittance intensity of the C–O–C group decreased with the BmimCl weight percentage. Sim et al. investigated IL in polymer blend electrolyte systems and claimed that the cation from the IL can coordinate at the polar atoms of the host polymer [42]. Therefore, the decrease of peak intensity can be explained by a strong interaction between the hydrogen group in the imidazolium ring of the $Bmim^+$ cation with the oxygen atoms from the host polymer.

Figure 3 demonstrate the intrinsic molecular interaction in the HGPEs, where the schematic diagrams show the interactions in the presence of BmimCl. The molecular interaction is important in polymer blends since it affects miscibility, in order to produce final products with desirable physical and chemical properties. It is noteworthy that the large size of the imidazolium cations had led to the weakening of the $Bmim^+$—Cl^- bonding, which will be broken and form a temporary partial bonding. According to Liew et al. [33], the hydrogen will be depronoted at NHC (2) of $Bmim^+$ to produce a stabilized (cation–-anion) pair which is known as carbene. After the deprotonation, there is a formation of a lone pair at the carbene, where the carbeneic carbon acts as the acceptor to the O–H hydrogen, producing a [C–-H–O]

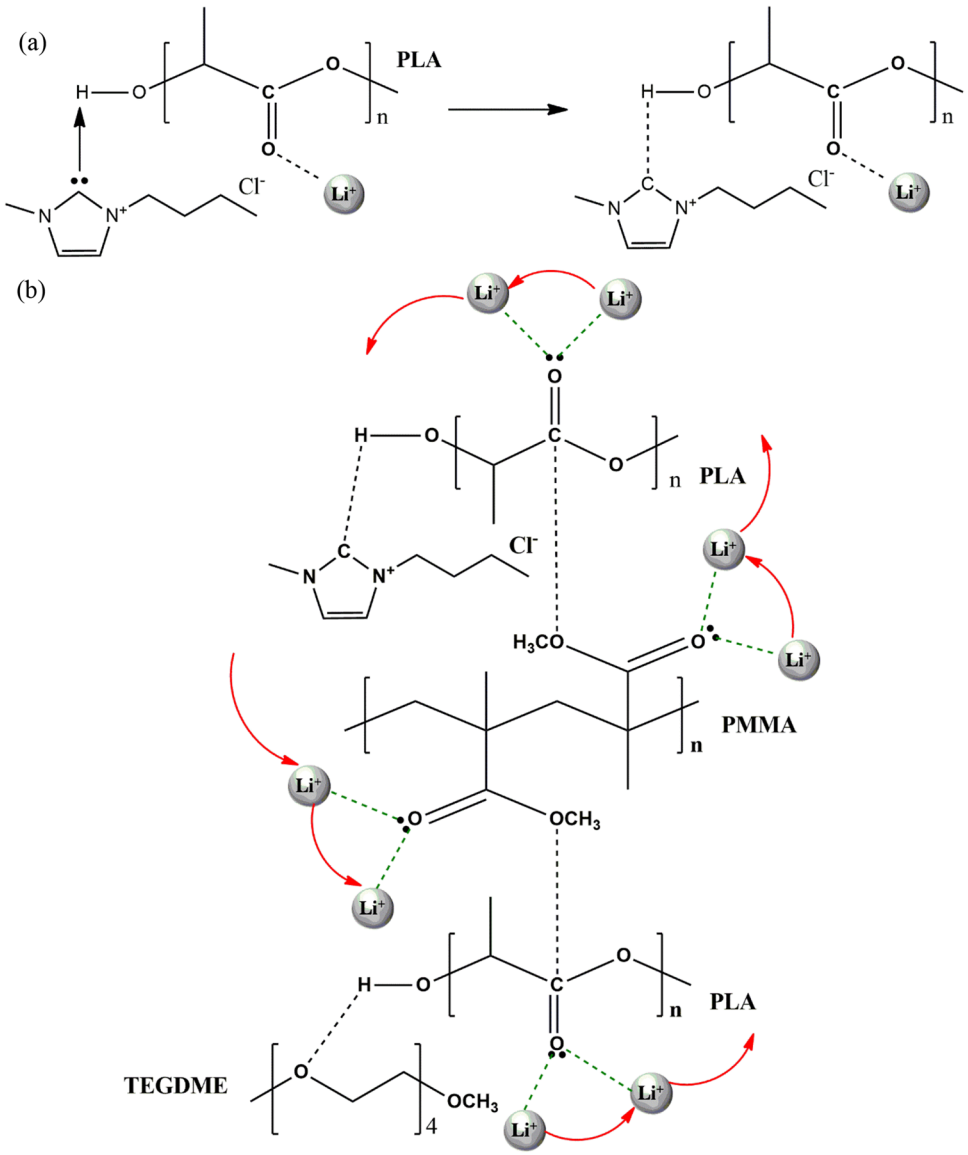

Fig. 3 Proposed schematic diagram of molecular interaction of (a) interaction of BmimCl with polymer host and (b) ion hopping in the HGPEs complex with BmimCl incorporation

of dipole pole interactions as presented in Fig. 3(a). This interaction results in the occurrence of carbocation. In this study, it was observed that the BmimCl could interact with PLA, whereas PMMA does not have potential for the atoms to attach to.

Meanwhile, Fig. 3(b) depicts the molecular interaction between the LiTFSI and BmimCl with the HGPEs. Notably, the PMMA and PLA have interacted via dipole–dipole forces due to the polar group of $–COCH_3$ in PMMA and C = O in PLA. This explanation corroborates the findings of previous research works [43]. Moreover, the solvent used (TEGDME) also plays an important role in the blending of both polymers and resulted in a homogenous system owing to the formation of dipole–dipole bonding through the interaction between the oxygen ether from the solvent with the hydrogen atom from PLA. The FTIR spectra evidenced these interactions that were discussed earlier. The addition of lithium salt has led to the ion dipole interaction at the C = O group of both PMMA and PLA, which causes those bonds to weaken through electron sharing and decreases electron density at the oxygen atoms [44]. The addition of BmimCl is therefore expected to primarily function as compartmentalization agents for the HPGEs, where it could improve the transport properties and hence enhance the conduction ability.

XRD analysis

Figure 4 demonstrates the XRD patterns of IL-based HGPEs at different BmimCl contents. Figure 4 shows a small sharp peak at 16° that is believed to belong to the crystalline phase of pure PLA [40]. Meanwhile, the broad peaks between

15–25° and 39–45° can be associated with the amorphous nature of PMMA [45]. The relative intensity of the broad peaks between 15–25° and 39–45° decreased with the increment of IL content for HGPE containing 5 to 15 wt.% BmimCl. These changes in diffraction intensities indicate that the amorphous nature of the hybrid GPE was improved when more BmimCl content was introduced into the system. This finding is in agreement with the previous work done by Syairah et al. [41], where they reported that adding IL into the system could reduce the degree of crystallinity, thus improving the amorphous behavior of the GPE. Furthermore, the decrement of crystallinity peaks could also be the result of coordination interactions between cations (Li^+ and $Bmim^+$) from LiTFSI and BmimCl, with the polymer host's ester oxygen atoms and hydrogen atoms, respectively. In addition, the polymeric chain in the amorphous phase is more flexible due to the decreased energy barrier, thus leading to the improvement of segmental motion in the polymer backbone [46, 47]. However, beyond 15 wt.% BmimCl, the increased crystalline peaks indicate ion aggregation of IL due to its high content [26].

To study in detail the amorphous nature of HGPEs, the characteristic peak due to the BmimCl was investigated by deconvoluting the XRD diffractogram of the HGPEs. Hafiza et al. [48] claimed that the degree of amorphous of polymer electrolytes can be measured by calculating the crystallinity degree. They also stated that a decreasing crystallinity percentage is a way to prove the improvement of the amorphousness of the polymer electrolytes. Figure 5 depicts the XRD deconvoluted spectrum of the PMMA-PLA-LiTFSI electrolyte with selected BmimCl content. From the deconvolution technique, the area under the graph of the crystalline peak and amorphous peak can be extracted and was used to calculate the degree of crystallinity via the following relation [49, 50]:

$$X_c = \frac{A_c}{A_c + A_a} \times 100\% \tag{3}$$

where X_c is degree of crystallinity in percentage. A_c is area under the peaks representing the total crystalline regions, while A_a denotes the area under the peaks representing the total amorphous region. The values of A_c, A_a, and X_c for selected HGPE system are listed in Table 1.

The calculated percentage of crystallinity revealed that adding BmimCl enhanced the amorphous phase of HGPEs. The deconvolution proved that the electrolyte containing 15 wt.% BmimCl was the most amorphous, with the lowest crystallinity degree of 23.89%. The complexation in the PMMA-PLA-LiTFSI-BmimCl matrixes was expected via intra- or inter-molecular interaction, which caused the polymer chain in the scattered structure to become more amorphous. However, the addition of BmimCl beyond 15 wt.% gave the opposite effect, where the crystallinity was increased. This increment in the degree of crystallinity might be due to the hybrid polymer host's inability to interact with excessive number of ions from the lithium salt or BmimCl, leading to the ions un-dissociating or re-associating. This situation limited the movement of ions, which subsequently caused the ionic conductivity to be reduced at high BmimCl content.

Complex impedance studies

Figure 6 portrays the complex impedance diagrams of IL-based HGPEs at different contents of BmimCl, in the range of 5 to 30 wt.%. The complex impedance plots reveal a straight

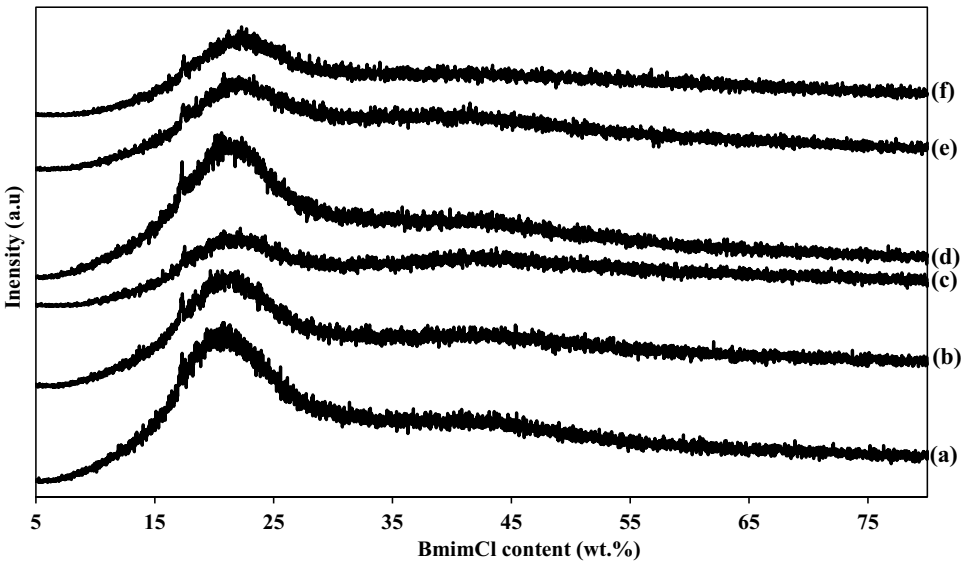

Fig. 4 XRD diffractograms of HGPEs at different BmimCl content of (a) 5 wt.%, (b) 10 wt.%, (c) 15 wt.%, (d) 20 wt.%, (e) 25 wt.%, and (f) 30 wt.%

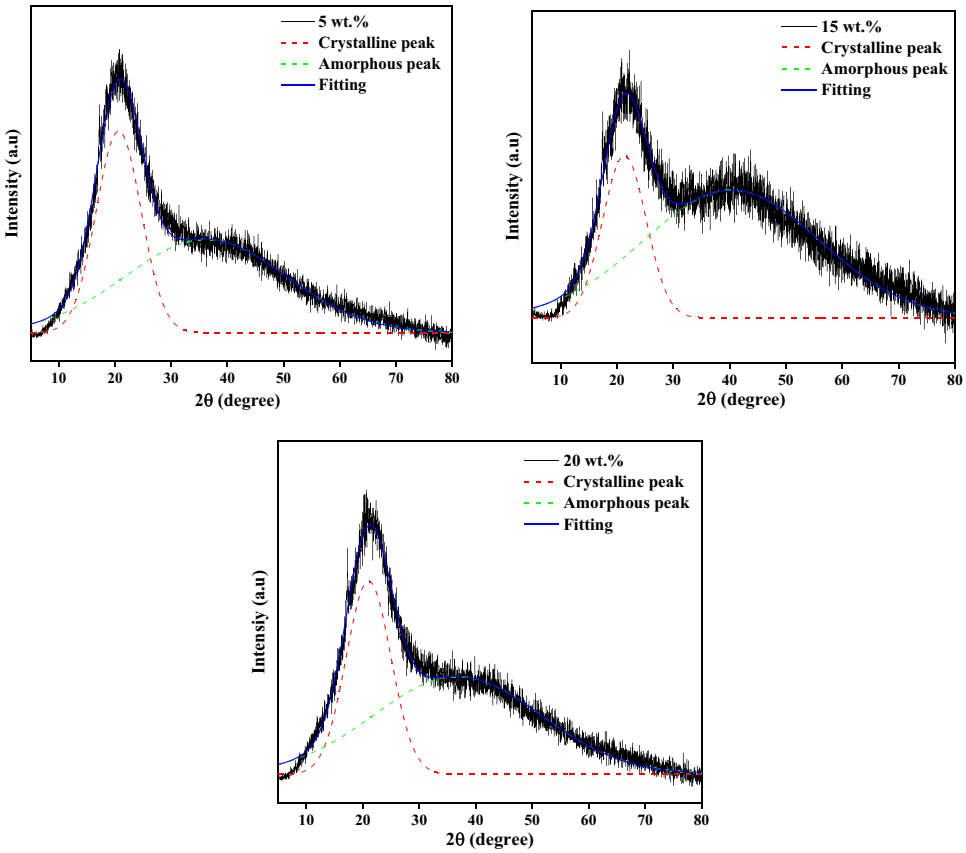

Fig. 5 Fitting XRD deconvolution for HGPEs containing 5 wt.%, 15 wt.%, and 20 wt.% BmimCl

Table 1 Crystallinity percentage of ionic liquid-based HGPEs

BmimCl content (wt.%)	A_c	A_a	X_c (%)
5	3971.39	6578.26	37.64
15	1561.59	4975.75	23.89
20	3450.98	6506.81	34.66

line parallel to the imaginary axis which may be attributed to the polarization effects between the electrode and electrolyte interface. In addition, the formation of a title spike can also be assigned to a combination in series between the bulk resistance, R_b, and constant phase element (CPE), also known as a "leaky capacitor." A similar observation was observed from a previous work [51]. The equation for fitting Cole–Cole plot was derived from the equivalent circuit presented in Fig. 6 which can be expressed as the following relation [26]:

$$Z' = R + \frac{\cos(\frac{\pi p}{2})}{C\omega^p} \tag{4}$$

$$Z'' = \frac{\sin(\frac{\pi p}{2})}{C\omega^p} \tag{5}$$

where R is denoted as bulk resistance, p is the deviation of plot from the axis, C is bulk capacitance of the present HGPEs system, while ω can be represented as angular frequency ($2\pi f$).

Furthermore, the presence of R_b could be elucidated from the migration of ions that occurred through the volume of the hybrid polymer matrix. Meanwhile, CPE exists due to the immobile polymer chains becoming polarized in the alternating field. The R_b value can be determined from the interception of the line with the real impedance axis [52]. Using the R_b value extracted from the impedance plot, the ionic conductivity value can be calculated. It is noticeable in the figure that the R_b value was found to decrease with the increase of ionic liquid content up to 15 wt.% and then started to rise again beyond that, which is believed to be related to the number of charge carriers and its mobility. The parameters for the circuit element of the HGPE systems at room temperature are listed in Table 2. The values for R_b fitting, k_2, and p were respectively obtained from the trial and error method to fit the present Cole–Cole plot using Eqs. 4 and 5. Based on the table, the lowest R_b value was observed for 15wt.% of BmimCl, indicating that it was the most conducting electrolyte compared to other IL contents.

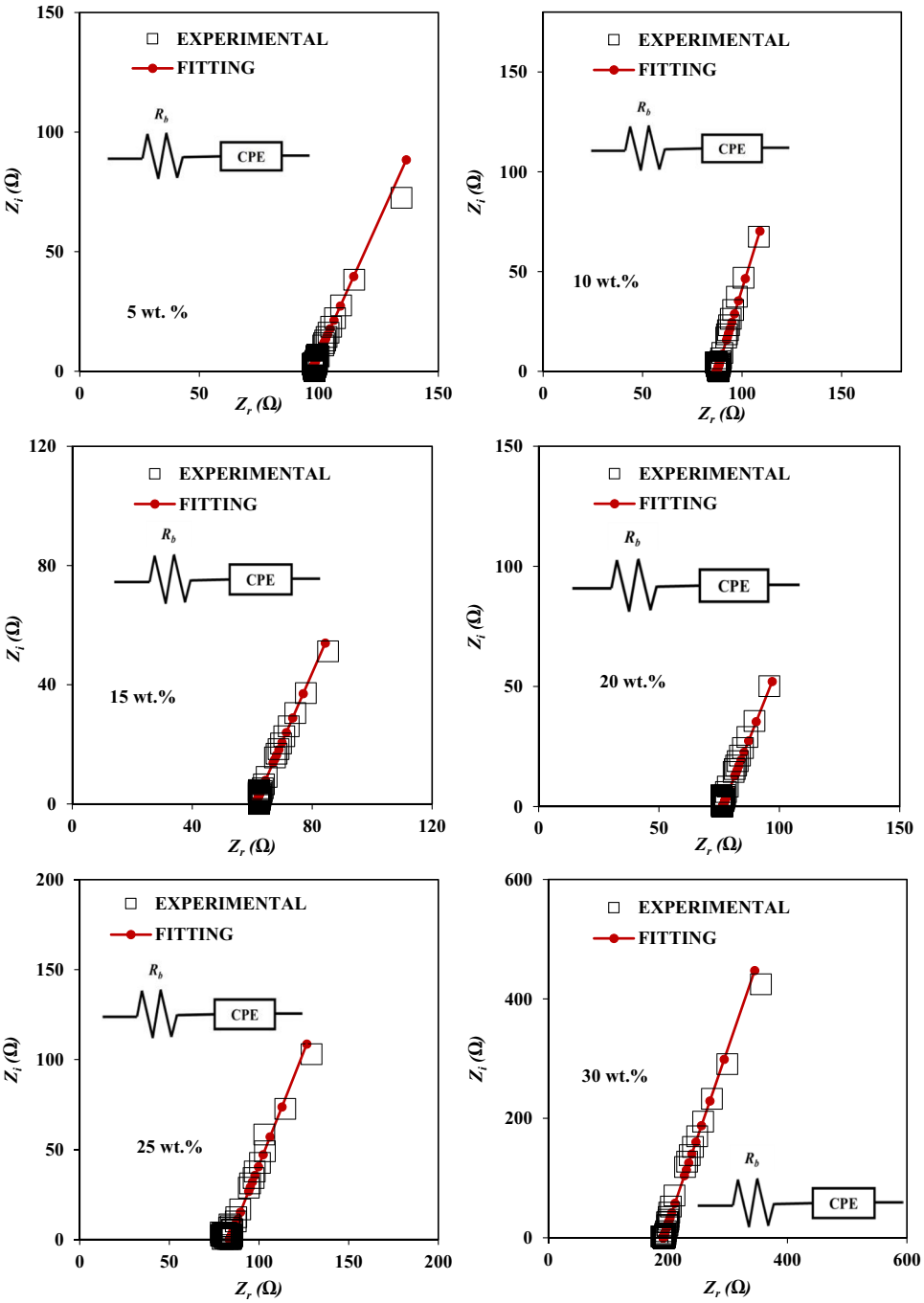

Fig. 6 Cole–Cole plot of various contents of BmimCl-based HGPEs at room temperature

Table 2 Fitting parameters for hybrid gel polymer electrolytes

BmimCl content (wt.%)	R_b *exp* (Ω)	R_b *fit* (Ω)	*k2* (*F* − *1*)	*p*
5	98.8	96.7	6.45×10^{3}	0.73
10	88.8	87.3	1.89×10^{4}	0.81
15	62.3	61.0	9.35×10^{3}	0.74
20	76.4	76.4	1.02×10^{4}	0.76
25	83.6	83.6	2.13×10^{4}	0.76
30	197.0	192.0	1.06×10^{5}	0.79

Ionic conductivity study

Figure 7 illustrates the plot of conductivity versus various contents of BmimCl in the hybrid GPEs. The figure shows that the ionic conductivity was improved when IL was incorporated into the HGPE system, but only up to 15 wt.% BmimCl. The enhanced ionic conductivity can be attributed to the changes in charge mobility and charge carrier concentrations. Moreover, the low viscosity of the IL enhanced the polymer flexibility chain, thus improving the segmental

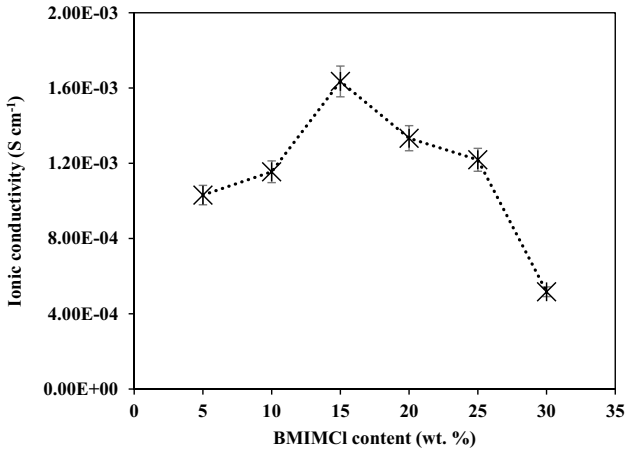

Fig. 7 The ionic conductivity of HGPEs at different wt.% BmimCl at room temperature

motion, which helps ions to move freely in the polymer backbone. Another property of the IL is the high dielectric constant that can promote the concentrations of charge carriers in the polymer electrolytes [53]. Another explanation is that the $Bmim^+$ cation (carbeneic carbon of imidazolium ring) interacted with the polar atoms from the hybrid host polymer, as discussed in the FTIR section. In the present system, four types of ions were detected, i.e., Li^+–-TFSI$^-$, and $Bmim^+$–-Cl^-, which contributed to the ionic conductivity. According to Azli et al. [34], BmimCl can act as a plasticizer that allows it to weaken the interaction between the hybrid host polymer and Li^+ ions from lithium salt. In this study, the maximum room temperature ionic conductivity of 1.63×10^{-3} S cm^{-1} was achieved for the IL-based HGPE system consisting of 15 wt.% BmimCl.

However, a further addition of 20 wt.% BmimCl has decreased the ionic conductivity to 1.33×10^{-3} S cm^{-1}. Incorporating 30 wt.% BmimCl has led to even lower conductivity, with a value of 5.17×10^{-4} S cm^{-1}. The reduction of ionic conductivity at high IL content can be ascribed to the formation of ion pairs and ion aggregates [54]. This phenomenon will lead to the creation of ion clusters, thus decreasing the number of free ions. In addition, the high BmimCl content provided more free ions, thus limiting the ability of ions to travel freely from one side to the other. This resulted in a decreased ionic conductivity as the ion mobility decreased [55].

Transport properties analysis

The variation in ionic conductivity as a function of the IL content can be understood on the basis of the number of mobile ions and ionic mobility. Thus, evaluating the quantitative ionic conductivity trend is necessary for a better insight into the ionic transport mechanism in polymer complexes and can also suggest ways for improvement. According to Arof et al. [51], the information obtained from the impedance analysis can be useful to investigate the characteristics of polymer electrolytes as well as their transport parameters in ionic conduction. Since this work only shows the equivalent circuit-based bulk resistance and bulk capacitance in series, the transport properties were determined using parameters obtained from the fitted Cole–Cole plot using the Arof-Noor (A-N) method. The diffusion coefficient, D, ionic mobility, μ, and number of ions, η, can be calculated from the following relation:

$$D = D_o exp^{[-0.0297(In(D_o))^2 - 1.4348(In(D_o)) - 14.504]} \tag{6}$$

where D_o is:

$$D_o = \frac{4{k_2}^4 d^2}{{R_b}^4 {\omega_2}^3} \tag{7}$$

where k_2 is capacitance ${k_2}^{-1}$ that was obtained from the fitting parameter, d is the thickness of the sample, R_b is the bulk resistance, and ω_2 is the angular frequency corresponding to the minimum imaginary impedance. Knowing the D value, the μ and η can be determined based on the following equations:

$$\mu = \frac{eD}{k_b T} \tag{8}$$

$$\eta = \frac{\sigma}{e\mu} \tag{9}$$

where e is the electric charge constant (1.602×10^{-19} C), K_b is the Boltzmann constant (1.38×10^{-23} J K^{-1}), and T is the absolute temperature.

The calculated transport parameters of IL-based HGPEs are plotted in the Fig. 8. It can be clearly seen that D and μ increased with the addition of BmimCl and this might be due to the variation of carrier content in the polymer complexes. The decreasing pattern of D and μ was observed when 15 wt.% BmimCl and higher were introduced into the system. At a high IL content, the dipole–dipole forces of the van der Walls interaction between the $Bmim^+$ in the medium increases, thus causing the ionic mobility to be reduced. In other words, the drop in D and μ values could be explained by the present electrolyte system being crowded with the free ions of $Bmim^+$—Cl^-. The overcrowding ions produce blocking pathways and limit the movement of ions between the coordinating sites in the polymer matrix. Meanwhile, the decrement of η at higher IL content is due to ions reassociating and forming neutral ion pairs. This finding further supports the trend of ionic conductivity and it can be concluded that the enhancement of ionic conductivity is mainly contributed from the D, μ, and η.

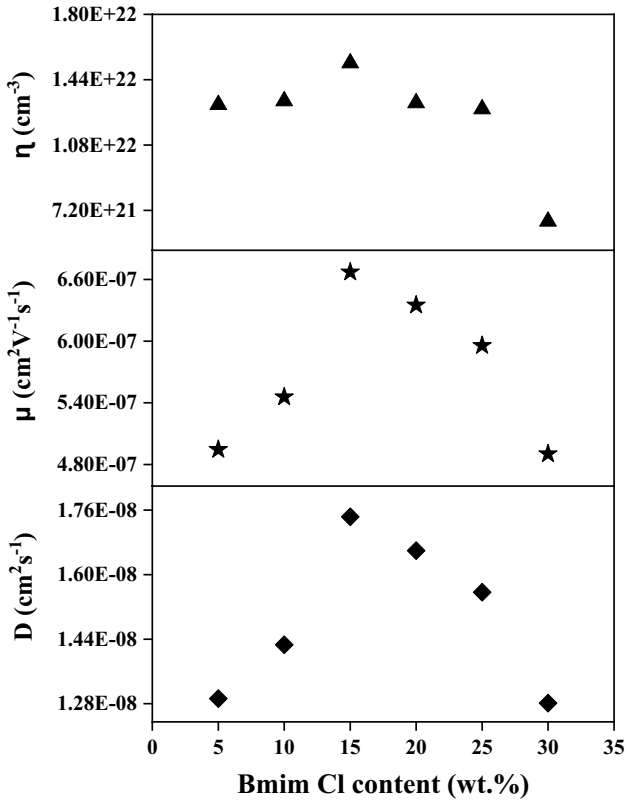

Fig. 8 Transport parameters for complexes of hybrid polymers with various BmimCl content

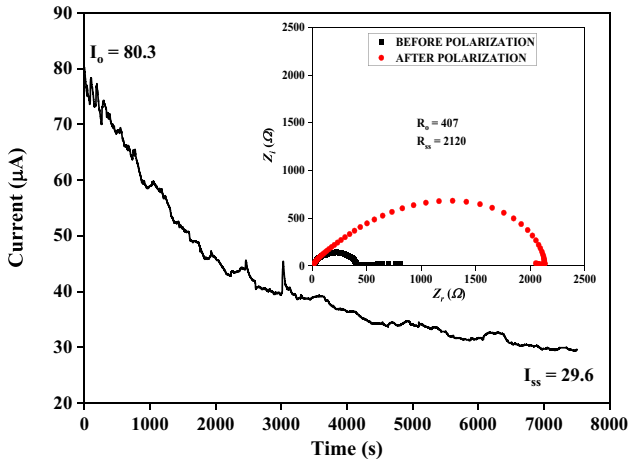

Fig. 9 The current–time curves of the dc polarization, while the insert figure shows impedance plots of hybrid gel polymer electrolytes containing 15 wt.% BmimCl before and after polarization, respectively

Lithium transference number measurement study

The lithium cation is the main charge that contributes during the charge discharged process in a lithium-ion battery. In addition, one of the properties of a good performing lithium-ion battery is an excellent ionic conductivity. There are four ionic species in the HGPE in this present work (Li^+, $TFSI^-$, $Bmim^+$, and Cl^-) that contribute to the total ionic conductivity. Therefore, it is necessarily to study the number of lithium ions in the IL-based HGPE system that influences the ionic conduction. The lithium-ion transference number (t_{Li}^+) for the IL-based HGPE system containing 15 wt.% BmimCl was calculated using combined ac impedance spectroscopy and dc polarization as shown in Fig. 9. From the insert in Fig. 9, the impedance spectroscopy was carried out to determine the film resistance before, R_o, and after, R_s polarization measurement. It can be seen from the plot of the polarization measurement that the R_s value was higher than the R_o. This is because during the polarization process, an electrochemical double layer was formed which led to the drop of initial current (I_o) with time and reached a steady-state (I_{ss}) where only a few ions were left passing through the cell as can be observed in Fig. 9 [56]. Moreover, Kufian et al. [38] argued the I_o is assigned as the total amount of mobile ions in the gel polymer electrolyte and it is believed that a higher t_{Li}^+ value will offer a higher I_o. Based on Eq. (2), the t_{Li}^+ was calculated for the highest conducting hybrid gel polymer electrolyte-based IL (15 wt.% BmimCl) and was found to be 0.67. In addition, a comparison of t_{Li}^+ values of different IL-based gel polymer electrolytes IL from previous works is plotted in Fig. 10. It can be clearly observed that the t_{Li}^+ value of the present study is comparable with the previous studies [37, 46, 57–59]. The migration of lithium ion in the gel polymer electrolyte is mainly attributed to the polymer host matrix polarity, which restricts large anion movement from the IL, thus providing pathways for Li^+ ions [37, 60]. Therefore, it can be expected that current study's IL-based HGPE system has the potential to show an excellent battery performance.

Potential windows study

For practical lithium-ion battery applications, evaluating the electrolyte's electrochemical stability within the battery system's operation potential is crucial. In this present work, the best performing IL-based hybrid gel polymer electrolyte was the 15 wt.% BmimCl, which was selected for the LSV measurement. Figure 11 shows the electrochemical stability of the IL-based HGPEs at ambient temperature at a scan rate of 10 mV s^{-1}. It can be observed from the figure that the decomposition of the electrolyte was at around 3.4 V and it rose gradually with the applied voltage. According to Liew et al. [61], the higher breakdown voltage may be attributed from good ionic conductivity. The authors also agreed that the incorporation of an IL contributes to an excellent rapid ion transport mechanism that helps ions to move smoothly in the polymer backbone, resulting in the higher charge

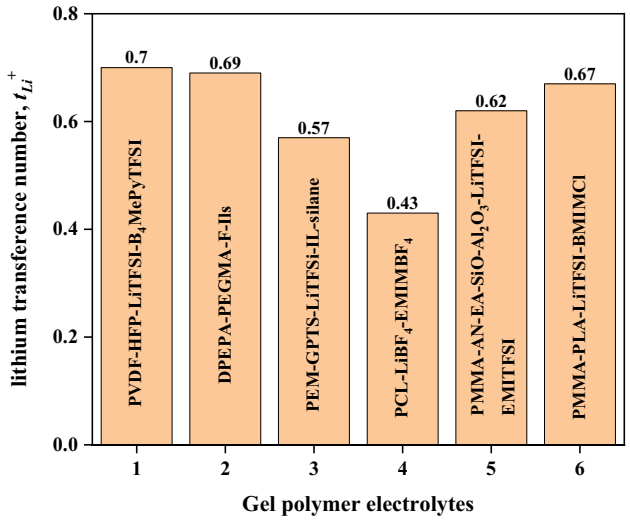

Fig. 10 A comparison of lithium transference values of IL-based gel polymer electrolytes from the present and previous works [37, 46, 57–59]

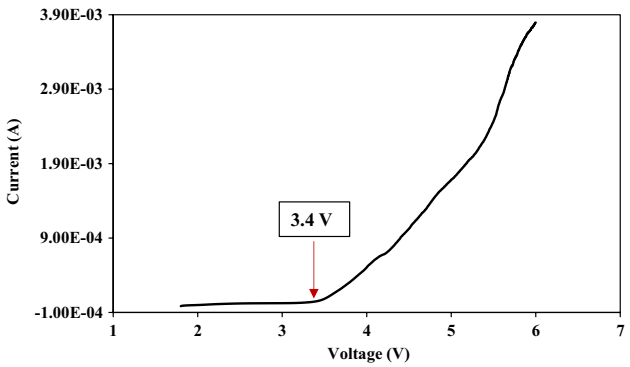

Fig. 11 Linear sweep voltammograms of the HGPEs incorporated with 15 wt.% BmimCl at a sweep rate of 10 mV s^{-1} at room temperature

accumulation at the electrode/electrolyte boundary. Table 3 lists the potential stability window of IL-incorporated gel polymer electrolytes from the literature. It can be observed that the value obtained in the present work is comparable with the previous LSV analyses. From our finding, it is believed that the blending of two polymer hosts can favor more volume sites for Li^+ and $Bmim^+$ ion coordination in the polymer backbone. Thus, it can be concluded that blending of the host polymer with other polymers could improve the breakdown voltage of polymer electrolytes.

Conclusion

A new hybrid gel polymer electrolyte based on PMMA blended with PLA, incorporated with LiTFSI, and doped with various contents of BmimCl has been successfully prepared and characterized. The physicochemical, conductivity, ionic transport, and electrochemical property studies have been performed and the conclusions are drawn accordingly. Analysis of FTIR indicated that there were interactions in the HGPE systems after the addition of BmimCl. The obvious complexations were observed to occur at the C-H, C = O, CH_3, and C–O–C groups. It is suggested that the changes in the HGPE structure was due to the interaction of the carbeniec carbon from the imidazolium group ($Bmim^+$) and Li^+ of the lithium salt with the hybrid polymer host's hydrogen atoms and ester oxygens, respectively. XRD analysis confirmed that adding BmimCl into the system reduced the degree of crystallinity, thus enhancing the amorphous behavior of the polymer electrolytes. Upon the incorporation of 15 wt.% of BmimCl in the PMMA-PLA-LiTFSI system, the electrical conductivity of the HGPEs increased and achieved the maximum value of 1.63×10^{-3} S cm^{-1}, corresponding to the lowest R_b value in the impedance plot. From the transport parameter studies, it can be clearly seen that the ionic conductivity is dependent on the diffusion coefficient, ionic mobility, and number of mobile ions. The lithium transference number was revealed to be high, at 0.67. The developed HGPE system also offers a wide electrochemical window of 3.4 V at room temperature. Based on all of the results obtained, this HGPE system incorporated with BmimCl could be a promising candidate for use as an electrolyte in flexible lithium-ion batteries.

Table 3 Previous electrochemical stability window studies of liquid electrolyte-based gel polymer electrolytes

Electrolyte	Ionic liquid	LSV (V)	References
PVDF-HFP-$TEABF_4$-EC-PC-BMIMCl	BMIMCl	2.4	[62]
PEO-NaI-MPII	MPII	1.9	[63]
PVDF-HFP-PMMA-$BMIMBF_4$	$BMIMBF_4$	4.5	[64]
PVC-PEMA-$Zn(OTf)_2$-EMIMTFSI	EMIMTFSI	3.23	[65]
PVDF-PMMA-LiTFSI-EMITFSI	EMIMTFSI	4.3	[66]
PMMA-PLA-LiTFSI-BMIMCl	BMIMCl	3.4	Current work

Funding The authors would like to thank University Malaysia Pahang (UMP) for providing financial support under the UMP Internal Grant (RDU 223304), Postgraduate Research Scheme (PGRS) No. UMP.05/26.10/03/PGRS210355 (University reference PGRS210355), Faculty of Industrial Sciences and Technology, UMP, and Centre for Ionics, University of Malaya, for the laboratory facilities as well as additional financial support from the Ministry of Higher Education (MOHE) under the Fundamental Research Grant Scheme (FRGS) (FRGS/1/2019/STG07/UMP/02/4) for the completion of this work.

References

1. Nayak PK, Yang L, Brehm W, Adelhelm P (2018) From lithium-ion to sodium-ion batteries: advantages, challenges, and surprises. Angew Chem Int Ed 57(1):102–120
2. Baskoro F, Wong HQ, Yen H-J (2019) Strategic structural design of a gel polymer electrolyte toward a high efficiency lithium-ion battery. ACS Appl Energy 2(6):3937–3971
3. Xu P, Chen H, Zhou X, Xiang H (2021) Gel polymer electrolyte based on PVDF-HFP matrix composited with rGO-PEG-NH_2 for high-performance lithium ion battery. J Membr Sci 617:118660
4. Wang J, Wang C, Wang W, Li W, Lou J (2022) Carboxymethylated nanocellulose-based gel polymer electrolyte with a high lithium ion transfer number for flexible lithium-ion batteries application. Chem Eng J 428:132604
5. Zhang P, Li R, Huang J, Liu B, Zhou M, Wen B, Xia Y, Okada S (2021) Flexible poly (vinylidene fluoride-co-hexafluoropropylene)-based gel polymer electrolyte for high-performance lithium-ion batteries. RSC Adv 11(20):11943–11951
6. Chen D, Lou Z, Jiang K, Shen G (2018) Device configurations and future prospects of flexible/stretchable lithium-ion batteries. Adv Funct Mater 28(51):1805596
7. Liu M, Jin B, Zhang Q, Zhan X, Chen F (2018) High-performance solid polymer electrolytes for lithium ion batteries based on sulfobetaine zwitterion and poly (ethylene oxide) modified polysiloxane. J Alloys Compd 742:619–628
8. Fenton D (1973) Complexes of alkali metal ions with poly (ethylene oxide). Polym 14:589
9. Mazuki NF, Fuzlin AF, Saadiah MA, Samsudin AS (2019) An investigation on the abnormal trend of the conductivity properties of CMC/PVA-doped NH_4Cl-based solid biopolymer electrolyte system. Ionics 25(6):2657–2667
10. Gu Y, Yang L, Luo S, Zhao E, Saito N (2022) A non-flammable, flexible and UV-cured gel polymer electrolyte with crosslinked polymer network for dendrite-suppressing lithium metal batteries. Ionics 28:3743–3759
11. Tu J, Wu K, Jiang J, Wu M, Hu Q, Xu G, Lou P, Zhang W (2021) A novel ceramic/polyurethane composite solid polymer electrolyte for high lithium batteries. Ionics 27(2):569–575
12. Tiwari R, Sonker E, Kumar D, Kumar K, Adhikary P, Krishnamoorthi S (2020) Preparation, characterization and electrical properties of alkali metal ions doped co-polymers based on TBF. J Mater Sci Eng, B 262:114687
13. Borah S, Sarmah JK, Deka M (2021) Understanding uptake kinetics and ion dynamics in microporous polymer gel electrolytes reinforced with SiO_2 nanofibers. J Mater Sci Eng, B 273:115419
14. Du Z, Su Y, Qu Y, Zhao L, Jia X, Mo Y, Yu F, Du J, Chen Y (2019) A mechanically robust, biodegradable and high performance cellulose gel membrane as gel polymer electrolyte of lithium-ion battery. Electrochim Acta 299:19–26
15. Liang S, Yan W, Wu X, Zhang Y, Zhu Y, Wang H, Wu Y (2018) Gel polymer electrolytes for lithium ion batteries: fabrication, characterization and performance. Solid State Ionics 318:2–18
16. Ngai KS, Ramesh S, Ramesh K, Juan JC (2016) A review of polymer electrolytes: fundamental, approaches and applications. Ionics 22(8):1259–1279
17. Vickraman P, Aravindan V, Shankarasubramanian N (2007) A study on the blending effect of polyvinyledene fluoride in the ionic transport mechanism of plasticized polyvinyl chloride+ lithium perchlorate gel polymer electrolytes. Ionics 13(5):355–360
18. Guo X, Li S, Chen F, Chu Y, Wang X, Wan W, Zhao L, Zhu Y (2021) Performance improvement of PVDF–HFP-based gel polymer electrolyte with the dopant of octavinyl-polyhedral oligomeric silsesquioxane. Materials 14(11):2701
19. Li L, Yang X, Li J, Xu Y (2018) A novel and shortcut method to prepare ionic liquid gel polymer electrolyte membranes for lithium-ion battery. Ionics 24(3):735–741
20. Long M-C, Wang T, Duan P-H, Gao Y, Wang X-L, Wu G, Wang Y-Z (2022) Thermotolerant and fireproof gel polymer electrolyte toward high-performance and safe lithium-ion battery. J Energy Chem 65:9–18
21. Pan Xr, Lian F, He Y, Peng Yf, Sun Xm, Wen Y, Guan Hy (2015) Enhanced mechanical strength and conductivity of PVFM based membrane and its supporting polymer electrolytes. J Appl Polym Sci 132(16):41839
22. Saxena P, Shukla P (2022) A comparative analysis of the basic properties and applications of poly (vinylidene fluoride) (PVDF) and poly (methyl methacrylate)(PMMA). Polym Bull 79:5635–5665
23. Kuppu SV, Jeyaraman AR, Guruviah PK, Thambusamy S (2018) Preparation and characterizations of PMMA-PVDF based polymer composite electrolyte materials for dye sensitized solar cell. Curr Appl Phys 18(6):619–625
24. Ramesh S, Liew C-W, Ramesh K (2011) Evaluation and investigation on the effect of ionic liquid onto PMMA-PVC gel polymer blend electrolytes. J Non-Cryst Solids 357(10):2132–2138
25. Zulkepely N, Majid S, Osman Z (2010) Effect of adding plasticizer on ionic conductivity and glass transition temperature of PMMA+ lithium iodide complexes. In: AIP Conference Proceedings, vol 1. American Institute of Physics, pp 205–208
26. Mazuki NF, Kufian MZ, Nagao Y, Samsudin AS (2022) Correlation studies between structural and ionic transport properties of lithium-ion hybrid gel polymer electrolytes based PMMA-PLA. J Polym Environ 30(5):1864–1879
27. Balo L, Gupta H, Singh VK, Singh RK (2017) Flexible gel polymer electrolyte based on ionic liquid EMIMTFSI for rechargeable battery application. Electrochim Acta 230:123–131
28. Wang Q-J, Zhang P, Wang B, Fan L-Z (2021) A novel gel polymer electrolyte based on trimethylolpropane trimethylacrylate/ionic liquid via in situ thermal polymerization for lithium-ion batteries. Electrochim Acta 370:137706
29. Ravi M, Kim S, Ran F, Kim DS, Lee YM, Ryou M-H (2021) Hybrid gel polymer electrolyte based on 1-methyl-1-Propylpyrrolidinium Bis (Trifluoromethanesulfonyl) imide for flexible and shape-variant lithium secondary batteries. J Membr Sci 621:119018
30. Bai J, Lu H, Cao Y, Li X, Wang J (2017) A novel ionic liquid polymer electrolyte for quasi-solid state lithium air batteries. J RSC advances 7(49):30603–30609
31. Mishra K, Rai DK (2021) Studies on ionic liquid based nanocomposite gel polymer electrolyte and its application in sodium battery. J Mater Sci Eng, B 267:115098

32. Balducci A, Jeong SS, Kim GT, Passerini S, Winter M, Schmuck M, Appetecchi GB, Marcilla R, Mecerreyes D, Barsukov V (2011) Development of safe, green and high performance ionic liquids-based batteries (ILLIBATT project). J Power Sources 196(22):9719–9730
33. Liew C-W, Ramesh S, Arof AK (2014) A novel approach on ionic liquid-based poly (vinyl alcohol) proton conductive polymer electrolytes for fuel cell applications. Int J Hydrogen Energy 39(6):2917–2928
34. Azli AA, Manan NSA, Kadir MFZ (2017) The development of Li^+ conducting polymer electrolyte based on potato starch/graphene oxide blend. Ionics 23(2):411–425
35. Latifi M, Ahmad A, Hassan NH, Kaddami H (2021) Carboxymethyl chitin doped 1-butyl-3-methylimidazolium chloride based solid polymer electrolyte. Mater, Today: Proceedings 36:16–21
36. Hor AA, Yadav N, Hashmi SA (2022) High energy density carbon supercapacitor with ionic liquid-based gel polymer electrolyte: role of redox-additive potassium iodide. J Energy Storage 47:103608
37. Tsao C-H, Su H-M, Huang H-T, Kuo P-L, Teng H (2019) Immobilized cation functional gel polymer electrolytes with high lithium transference number for lithium ion batteries. J Membr Sci 572:382–389
38. Kufian MZ, Ramesh S, Arof AK (2021) PMMA-LiTFSI based gel polymer electrolyte for lithium-oxygen cell application. Opt Mater 120:111418
39. Bruce PG, Vincent CA (1987) Steady state current flow in solid binary electrolyte cells. J Electroanal Chem Interf Electrochem 225(1–2):1–17
40. Mazuki NF, Nagao Y, Kufian MZ, Samsudin AS (2020) The influences of PLA into PMMA on crystallinity and thermal properties enhancement-based hybrid polymer in gel properties. Mater, Today: Proceedings 49(8):3105–3111
41. Ghani NAA, Anuar FH, Ahmad A, Mobarak NN, Shamsudin IJ, Dzulkipli MZ, Hassan NH (2020) Incorporating 1-butyl-3-methylimidazolium chloride ionic liquid into iota carrageenan solid biopolymer electrolyte for electrochemical devices application. Sains Malaysiana 49(2):305–313
42. Sim LN, Majid SR, Arof AK (2014) Effects of 1–butyl–3–methyl imidazolium trifluoromethanesulfonate ionic liquid in poly (ethyl methacrylate)/poly (vinylidenefluoride–co–hexafluoropropylene) blend based polymer electrolyte system. Electrochim Acta 123:190–197
43. Teoh EL, Chow WS (2018) Transparency, ultraviolet transmittance, and miscibility of poly (lactic acid)/poly (methyl methacrylate) blends. J Elastomers Plast 50(7):596–610
44. Mendes-Felipe C, Barbosa JC, Gonçalves R, Miranda D, Costa CM, Vilas-Vilela JL, Lanceros-Mendez S (2021) Lithium bis (trifluoromethanesulfonyl) imide blended in polyurethane acrylate photocurable solid polymer electrolytes for lithium-ion batteries. J Energy Chem 62:485–496
45. Gohel K, Kanchan DK (2019) Effect of PC: DEC plasticizers on structural and electrical properties of PVDF–HFP: PMMA based gel polymer electrolyte system. J Mater Sci Mater Electron 30(13):12260–12268
46. Ravi M, Song S, Wang J, Wang T, Nadimicherla R (2016) Ionic liquid incorporated biodegradable gel polymer electrolyte for lithium ion battery applications. J Mater Sci Mater Electron 27(2):1370–1377
47. Polu AR, Rhee H-W (2017) Ionic liquid doped PEO-based solid polymer electrolytes for lithium-ion polymer batteries. Int J Hydrogen Energy 42(10):7212–7219
48. Hafiza MN, Isa MIN (2017) Solid polymer electrolyte production from 2-hydroxyethyl cellulose: effect of ammonium nitrate composition on its structural properties. Carbohydr Polym 165:123–131
49. Vo DT, Do HN, Nguyen TT, Nguyen TTH, Okada S, Le MLP (2019) Sodium ion conducting gel polymer electrolyte using poly (vinylidene fluoride hexafluoropropylene). J Mater Sci Eng, B 241:27–35
50. Zainuddin NK, Saadiah MA, Abdul Majeed APP, Samsudin AS (2018) Characterization on conduction properties of carboxymethyl cellulose/kappa carrageenan blend-based polymer electrolyte system. Int J Polym Anal Charact 23(4):321–330
51. Arof AK, Amirudin S, Yusof SZ, Noor IM (2014) A method based on impedance spectroscopy to determine transport properties of polymer electrolytes. PCCP 16(5):1856–1867
52. Sikkanthar S, Karthikeyan S, Selvasekarapandian S, Arunkumar D, Nithya H, Junichi K (2016) Structural, electrical conductivity, and transport analysis of PAN–NH_4Cl polymer electrolyte system. Ionics 22(7):1085–1094
53. Farah N, Ng HM, Numan A, Liew C-W, Latip NAA, Ramesh K, Ramesh S (2019) Solid polymer electrolytes based on poly (vinyl alcohol) incorporated with sodium salt and ionic liquid for electrical double layer capacitor. J Mater Sci Eng, B 251:114468
54. Tu Q-M, Fan L-Q, Pan F, Huang J-L, Gu Y, Lin J-M, Huang M-L, Huang Y-F, Wu J-H (2018) Design of a novel redox-active gel polymer electrolyte with a dual-role ionic liquid for flexible supercapacitors. Electrochim Acta 268:562–568
55. Fuzlin AF, Misnon II, Nagao Y, Samsudin AS (2022) Study on ionic conduction of alginate bio-based polymer electrolytes by incorporating ionic liquid. Mater Today: Proc 51(2):1455–1459
56. Khoon LT, Fui M-LW, Hassan NH, Su'ait MS, Vedarajan R, Matsumi N, Bin Kassim M, Shyuan LK, Ahmad A (2019) In situ sol–gel preparation of ZrO_2 in nano-composite polymer electrolyte of PVDF-HFP/MG49 for lithium-ion polymer battery. J Sol-Gel Sci Technol 90(3):665–675
57. Yang P, Liu L, Li L, Hou J, Xu Y, Ren X, An M, Li N (2014) Gel polymer electrolyte based on polyvinylidenefluoride-co-hexafluoropropylene and ionic liquid for lithium ion battery. Electrochim Acta 115:454–460
58. Zhou T, Zhao Y, Choi JW, Coskun A (2021) Ionic liquid functionalized gel polymer electrolytes for stable lithium metal batteries. Angew Chem Int Ed 133(42):22973–22978
59. Li M, Liao Y, Liu Q, Xu J, Sun P, Shi H, Li W (2018) Application of the imidazolium ionic liquid based nano-particle decorated gel polymer electrolyte for high safety lithium ion battery. Electrochim Acta 284:188–201
60. Karuppasamy K, Reddy PA, Srinivas G, Tewari A, Sharma R, Shajan XS, Gupta D (2016) Electrochemical and cycling performances of novel nonafluorobutanesulfonate (nonaflate) ionic liquid based ternary gel polymer electrolyte membranes for rechargeable lithium ion batteries. J Membr Sci 514:350–357
61. Liew C-W, Ramesh S, Arof A (2015) Characterization of ionic liquid added poly (vinyl alcohol)-based proton conducting polymer electrolytes and electrochemical studies on the supercapacitors. Int J Hydrogen Energy 40(1):852–862
62. Tripathi M, Tripathi SK (2017) Electrical studies on ionic liquid-based gel polymer electrolyte for its application in EDLCs. Ionics 23(10):2735–2746
63. Syairah A, Khanmirzaei MH, Saidi NM, Farhana NK, Ramesh S, Ramesh K (2019) Effect of different imidazolium-based ionic liquids on gel polymer electrolytes for dye-sensitized solar cells. Ionics 25(5):2427–2435
64. Zhai W, Zhu H-j, Wang L, Liu X-m, Yang H (2014) Study of PVDF-HFP/PMMA blended micro-porous gel polymer electrolyte incorporating ionic liquid [BMIM] BF_4 for Lithium ion batteries. Electrochim Acta 133:623–630

65. Prasanna CM, Suthanthiraraj SA (2016) Effective influences of 1-ethyl-3-methylimidazolium bis (trifluoromethylsulfonyl) imide (EMIMTFSI) ionic liquid on the ion transport properties of microporous zinc-ion conducting poly (vinyl chloride)/poly (ethyl methacrylate) blend-based polymer electrolytes. J Polym Res 23(7):1–17
66. Yusoff NFM, Idris N (2017) Ionic liquid based PVDF/PMMA gel polymer electrolyte for lithium rechargeable battery. J Mech Eng Sci 11:3152–3165

Publisher's Note Springer Nature remains neutral with regard to jurisdictional claims in published maps and institutional affiliations.

Springer Nature or its licensor (e.g. a society or other partner) holds exclusive rights to this article under a publishing agreement with the author(s) or other rightsholder(s); author self-archiving of the accepted manuscript version of this article is solely governed by the terms of such publishing agreement and applicable law.